



ELSEVIER

Contents lists available at ScienceDirect

Physica B

journal homepage: www.elsevier.com/locate/physb

DSC, TGA and dielectric properties of carboxymethyl cellulose/polyvinyl alcohol blends

S. El-Sayed^{b,*}, K.H. Mahmoud^{a,c}, A.A. Fatah^{a,c}, A. Hassen^{a,b}

^a Physics Department, Faculty of Science and Education, Taif University, Saudi Arabia

^b Physics Department, Faculty of Science, Fayoum University, 63514 El Fayoum, Egypt

^c Physics Department, Faculty of Science, Cairo University, Giza, Egypt

ARTICLE INFO

Article history:

Received 11 March 2010

Received in revised form

23 July 2011

Accepted 25 July 2011

Available online 30 July 2011

Keywords:

Carboxymethyl cellulose

Polyvinyl alcohol

Blends

Thermal analysis

Dielectric properties

Hopping conduction mechanism

ABSTRACT

Films with different compositions of polyvinyl alcohol (PVA) and carboxymethyl cellulose (CMC) blends have been prepared using the casting method. Differential scanning calorimetry (DSC), thermogravimetric analysis (TGA) and dielectric spectroscopy of all compositions have been investigated. It was found that PVA and CMC are compatible in the studied range of composition. With increasing CMC content, the thermal stability of PVA increases. Based on DSC and TGA data, the activation energies of all the investigated samples were calculated. The absorption edge (E_a) was also determined from Ultraviolet–visible (UV–vis) spectra.

Dielectric permittivity, loss tangent and ac conductivity of all samples were studied as functions of temperature and frequency. The results show that the dielectric dispersion consists of both dipolar and interfacial polarization. The frequency dependence of the ac conductivity indicates that the correlated barrier hopping (CBH) is the most suitable mechanism for conduction. The polaron binding energy (U_M) was determined. Results of the present system are compared with those of similar materials.

© 2011 Elsevier B.V. All rights reserved.

1. Introduction

Polymer blends were recommended in the last few decades as the most promising way to prepare new material with tailored individual properties. Blending of existing commodity or engineering polymers can often be implemented more rapidly than realization of new polymer chemistry including development of monomer synthesis and polymerization technology. Therefore, copolymers have been extensively studied because of their high potential of application, as well as their significance in basic science. It is also known that the dielectric constant and the dissipation factor of these materials as a function of temperature and frequency are crucial quantities required in the design of devices. They reveal information on the chemical and physical states of polymers.

Carboxymethyl cellulose (CMC), one of the important cellulose derivatives, is generally prepared through the reaction of alkali cellulose with monochloroacetate or its sodium salt in organic medium. CMC possesses many desirable qualities, such as filming, emulsification, suspension, water maintaining, bind and inspissations. Therefore, it is used for many applications such as in

medicine, food, textures, toilet, electrical elements, paper making, printing and dyeing. On the other hand, polyvinyl alcohol (PVA) is also one of the promising representatives of polymeric material. There are many proposals for its applications such as paper coating, textile sizing, flexible water-soluble packing films owing to its high clarity and excellent durability. In addition, PVA is not only thermally stable over a wide range of temperature (173–473 K) [1] but also used in the production of polarizing sheets [2]. These and other applications stimulate an interest in improving various properties of PVA by blending with other polymers, in particular with natural polymers or synthetically modified natural polymers such as CMC.

Thermal analysis, such as DSC and TGA are frequently used to describe the behavior of a sample as a function of temperature. DSC and TGA are capable of revealing thermal transitions, degradation processes and thermal stability studies. Moreover, dielectric investigations [3–10] are of special interest in relation to polymers because they provide detailed information on the molecular configurations. A dielectric relaxation of polymeric materials is useful to understand the flexibility of the polymer segments and internal group rotations.

DSC of PVA/methyl cellulose (MC) blends revealed that PVA crystallinity in PVA hydrogel decreased drastically with increasing MC content and crosslinking [11]. Satri and Scandola [12] studied the viscoelastic and thermal properties of collagen/PVA blends. They concluded that the examined binary blends are

* Corresponding author at: Physics Department, Faculty of Science and Education, Taif University, Saudi Arabia. Tel.: +966543710664; fax: +96628321071.

E-mail address: somyia.elsayed@yahoo.com (S. El-Sayed).

heterogeneous systems and composed of pure polymer phases. This means that PVA is thermodynamically immiscible with collagen.

A dielectric study of CMC [13] and PVA [14,15] in aqueous solutions has been reported. The dielectric properties of CMC are very similar to those of other polyelectrolytes and the electric structure is unipolar rather than dipolar. In the case of PVA, the polymer chain is very flexible due to either intra- or inter-molecular associations. This flexibility of the chain in PVA varies monotonically with temperature. Moreover, there is a large contribution of segmental motion and group rotations to the relaxation processes in PVA flexible chain through the formation of hydrogen bonds with the solvent water.

Since the synthesis of polymer blends show various physical properties and potential technological applications, a great number of investigations were carried out [16–21]. The thermal sampling (TS) technique of PVA/sodium carboxymethyl cellulose, NaCMC, indicates that the relaxation phenomenon in these blends may be ascribed to glass-like transition [16]. Also, the dipoles of PVA/NaCMC blend become oriented with applied electric field. Both ac and dc conductivity of polyaniline–polyvinyl alcohol blends were reported [17]. The results show that the temperature dependence of the dc conductivity in these materials follows variable range hopping (VRH) conduction. On the other hand, the behavior of ac conductivity obeys ω^s power law and can be interpreted according to the correlated barrier hopping (CBH) model.

The electrical properties of polyaniline (PANI) and CMC composites [18] are different compared to those of PVA–polyethylene (PE) copolymers [19]. In the first samples, the conductivity data can be fitted well by the percolation theory, $\sigma(f) = C(f - f_c)^t$, where $\sigma(f)$ is the experimentally obtained conductivity measured at room temperature, C is constant, t is the critical exponent and f is the volume fraction of filler particles. In PVA–PE copolymer, the dielectric relaxation is invariably attributed to dipolar and space charge polarization.

It is expected to obtain from PVA and CMC polymers new compositions of desired properties. The method used to improve the physical properties of some polymers is to blend it with others within the same solvent. This method facilitates the preparation of composites for special applications by changing the degree of crystallinity of the polymer and controlling the impeded amorphous regions in PVA. Also the blend can change the ionization of CMC. These new blends increase the industrial applications of polymers. The aim of the present work is to study the electrets, which are formed from the blending of PVA by CMC. This study includes characterization techniques such as DSC, TGA and absorption edge in order to reveal the information about miscibility of these blends. Dielectric spectra were also performed to shed light on dynamics of entities having dipole reorientation, rotations of the main and segmental chains and conductivity mechanisms.

2. Experimental work and techniques

Polyvinyl alcohol (PVA) of molecular weight of approximately 17,000 and carboxymethyl cellulose (CMC) of molecular weight of approximately 250,000 were supplied by BDH chemical Ltd Poole England Company. The solution method was employed to obtain film samples. Weighed amounts of natural granules PVA were dissolved in a mixture of distilled water and ethanol in ratio 4:1. Also, weighed amounts of CMC were dissolved in distilled water at room temperature. Solutions of PVA/CMC were mixed together with different weight percentage 100/0, 80/20, 50/50, 20/80 and 0/100 (wt/wt%). Complete dissolution was obtained using a magnetic stirrer at 50 °C on water bath for 3 h. Films of appropriate thickness ($\sim 60 \mu\text{m}$) were cast onto stainless steel Petri dishes, and then dried in air at room temperature until the

Table 1
The notations of the PVA/CMC (wt/wt%) blend samples.

PVA/CMC (wt/wt%)	Sample notation
100/0	S ₁
80/20	S ₂
50/50	S ₃
20/80	S ₄
0/100	S ₅

solvent was evaporated. Films were cut into square pieces of side 1.0 cm. Notations of sample compositions were used as listed in Table 1.

The UV–vis absorption spectra were measured in the wavelength range 200–800 nm using PERKIN ELMER 4B spectrophotometer. Thermal analysis was carried out using a computerized differential scanning calorimetry (DSC) and thermogravimetric analysis (TGA), T_{A-50} Schimadza Corporation, Kyoto, Japan. Measurements were carried out under nitrogen atmosphere (30 ml/min). Measurements of dielectric constant (ϵ') and loss tangent factor ($\tan \delta$) were carried out using a programmable automatic RLC meter (Type PM.6304/031). The ac electrical conductivity, σ_{ac} , was obtained using the relation ($\sigma_{ac} = \omega \epsilon_0 \epsilon'' \tan \delta$). The measured samples show reproducible behaviors and the accuracy of the data of ϵ' and $\tan \delta$ was about $\pm 2\%$.

3. Results and discussions

3.1. UV–vis spectrum

UV–vis analysis gives evidence for understanding energy band diagram and optical parameters, which are affected by the processing conditions. The absorption edge values were determined from the plot of the absorption coefficient, $\alpha(\nu)$, as in Eq. (1), with the incident photon energy ($h\nu$) for individual PVA and CMC and their blends in the UV–vis region. The absorption coefficient $\alpha(\nu)$ of the optical absorption can be calculated from the relation

$$\alpha(\nu) = \frac{B}{d} \quad (1)$$

where d is the thickness of the sample and B is the absorbance. The calculated values of $\alpha(\nu)$ are relatively small ($10\text{--}160 \text{ cm}^{-1}$) as in most low carrier concentration materials. Based on Urbach formula [22], where the absorption coefficient $\alpha(\nu)$ of the optical absorption near the band edge for many amorphous materials shows an exponential dependence on photon energy ($h\nu$) is as follows:

$$\alpha(\nu) = \alpha_0 \exp\left(\frac{h\nu}{\Delta E}\right) \quad (2)$$

where α_0 is constant and ΔE is the width of the band tails of the localized states in normally forbidden band gaps associated with the amorphous nature of the materials. The extrapolation of the linear portion of the $[\alpha(\nu) - h\nu(\text{eV})]$ curves (not shown here) to the abscissa has been used to find the values of the absorption edge (E_a). The values of E_a are listed in Table 2. It is clear that the values of E_a for the blend samples are less than those for the homopolymers (S₁ and S₅). This may reflect the induced changes in the number of available final states according to the blend composition. In addition, S₃ [50/50 (wt/wt%) of PVA/CMC] has the smallest absorption edge (2.5 eV) indicating that it has a higher carrier concentration in the localized levels as compared to other samples.

Table 2

The absorption edge (E_a), glass phase transition (T_g), melting phase transition (T_m) and associated enthalpies (ΔH) of PVA/CMC blend samples.

Melting phase transition (T_m)		Glass phase transition (T_g)		Absorption edge	Sample
ΔH (J/g)	T_m (°C)	ΔH (J/g)	T_g (°C)	E_a (eV)	
50	218.5	72	87	2.81	S ₁
44	217.8	79	92	2.75	S ₂
26	217.4	85	102	2.50	S ₃
9.2	221.0	196	80	2.70	S ₄
–	–	121	75	2.92	S ₅

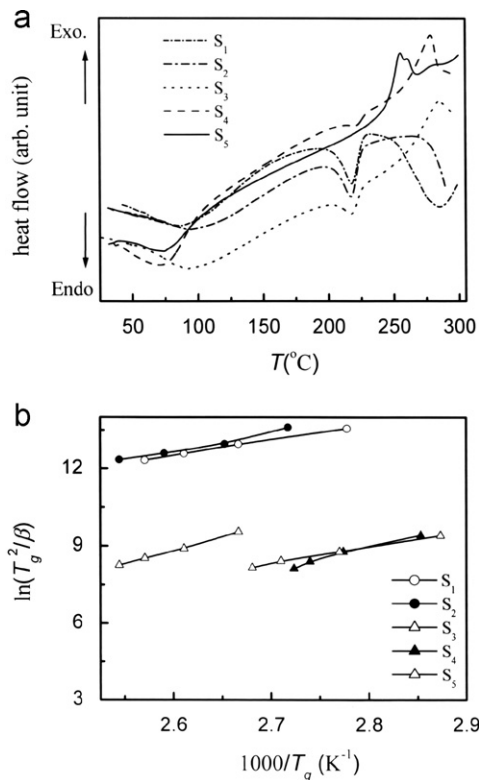


Fig. 1. (a) DSC thermogram during heating of all the blend samples. $\ln(T_g^2/\beta)$ (K^{-1}) versus $1000/T_g$ (K^{-1}) of PVA/CMC blends.

3.2. Thermal analysis

3.2.1. Differential scanning calorimetry (DSC)

DSC is capable of revealing first and second order thermal transitions like melting (T_m), crystallization (T_c) and glass transition (T_g) phenomena. Fig. 1(a) shows the heating run of PVA/CMC blend samples up to 300 °C. For PVA homopolymer (sample S₁), DSC displays an endothermic glass transition peak around 87 °C with an enthalpy change of $\Delta H \approx 72$ J/g. Another sharp endotherm melting transition at 218 °C with $\Delta H \approx 50$ J/g is observed. The heat required for melting of 100% crystalline S₁ is 138.6 J/g [20]. Thus the nominal value of crystallinity obtained from the DSC thermogram of S₁ is about 37%. The relatively weak and broadened glass transitions can be ascribed to the semicrystalline nature of the material. The values of T_g and T_m are in agreement with those in previous reports [21,23,24]. DSC thermogram of S₅ shows a relatively broad endotherm glass transition around 75 °C and exothermic crystalline transition at 278 °C. The change of the enthalpies of the glass and crystalline transitions are 121.0 and 3.61 J/g, respectively. The temperatures of the

phase transitions as well as the change of the enthalpies of the investigated samples are listed in Table 2.

It is also interesting to estimate how the thermal transition of PVA varied after being mixed with different concentrations of CMC. Both S₁ and S₅ possess T_g that is near to each other, and therefore, the assessment of transitions behavior in the PVA/CMC blend samples had to be made carefully. As seen in Fig. 1(a), DSC scan for S₃ shows three transitions peaks. Two peaks are endothermic at 93 and 218 °C with enthalpies, ΔH , of 85 and 26 J/g, respectively, and one exothermic peak at 284 °C with $\Delta H \approx 44$ J/g. The transition peaks appearing at 218 and 284 °C can be attributed to the melting and the crystallization transitions of PVA and CMC, respectively. However, the broad glass transition peak that appeared around 101 °C may be due to the overlapping T_g transitions of the two polymer blend samples. It is also noted that the enthalpy associated with endotherm melting transition decreased with decreasing PVA content while the peak position remained approximately unaltered. The tendency of an apparent disproportional reduction in enthalpy with a decrease of PVA content implies a rapid decrease of the degree of crystallinity of PVA due to mixing with CMC [25]. The intensity and enthalpy associated with exothermic crystalline peak increased with decreasing PVA content in the blend samples, while its position is approximately unaffected. In addition, the enthalpy of the glass transition peak irregularly changed with increasing concentration of CMC in the blend samples. The position of the glass transition temperature T_g shifts toward higher temperatures as the content of CMC increases up to 50 wt%. Accordingly, these observations indicate the compatibility between CMC and PVA because of the presence of –OH and CH₂OCH₂COONa in CMC and –OH groups in PVA capable of hydrogen bonding.

The activation energy of enthalpy relaxation across the glass transition or the activation energy of the glass transition, E_g , can be obtained using Kissinger's relation, which was derived for the crystallization process [26,27]:

$$\ln\left(\frac{T_g^2}{\beta}\right) = \frac{E_g}{RT_g} + c \quad (3)$$

where R is the universal gas constant, β is the heating rate and c is a constant. The values of E_g were derived from the plot of $\ln(T_g^2/\beta)$ versus $1000/T_g$, which exhibits a straight line of slope E_g/R as shown in Fig. 1(b). The values of the activation energies, E_g , are 51, 62, 91, 79 and 54 kJ mol⁻¹ for S₁, S₂, S₃, S₄ and S₅, respectively. It is observed that E_g increases as the CMC content increases up to 50 wt% and then decreases. The increasing value of E_g may be attributed to the increase of T_g and packing structure [28]. For the sake of brevity, Fig. 2(a–c) depicts the variation of T_g with the heating rate β for S₁, S₃ and S₅. As seen, T_g shifts to higher temperatures with increasing heating rate. On the other hand, T_m is only slightly affected with the increase of β . Moreover, the exothermic peak of S₅ shifts toward higher temperatures with increasing β .

3.2.2. Thermogravimetric analysis (TGA)

Thermogravimetric analysis (TGA) is a process in which a material is decomposed by heat, which causes bonds within the molecule to be broken. TGA plays an important role in determining thermal stability of the materials. TGA curves and their derivatives DrTGA of S₁, S₂ and S₃ are presented in Fig. 3(a–c) while the curves of S₄ and S₅ are displayed in Fig. 3(d,e). The TGA curves show that the thermal stability of the blend samples changes with increasing CMC content and the degradation is completed in two steps. These steps are distinguishable in the diagram of mass loss (TGA%) during heating as well as more clearly- in the diagram of derivative mass loss (DrTGA). All the

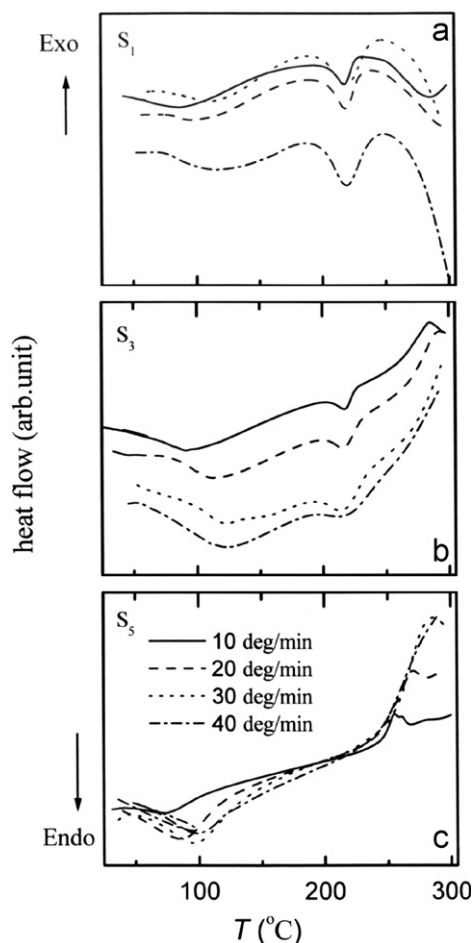


Fig. 2. DSC thermogram at different heating rates of (a) S_1 , (b) S_3 and (c) S_5 .

samples show a small (5–15%) mass loss for the first decomposition step and more significant mass loss (39–75%) for the second step. Table 3 shows the decomposition steps and percentage mass loss for individual polymers and their blends. The lower values of percentage mass loss in the first decomposition step may be due to the evaporation of bound water [29]. The latter process in TGA curves covers the melting point of PVA and the thermal degradation of the samples. Therefore the higher values of the mass loss in the second decomposition step may be attributed to the degradation of side chain and the loss of CO_2 in the case of CMC. In addition, DrTGA curves show two broad temperature peaks corresponding to the first and second decomposition

Table 3
TGA and DrTGA data and the activation energies (according to Eq. 5) for PVA/CMC blends.

Sample	Region of decomposition	E (kJ mol^{-1})	Temperature ($^{\circ}\text{C}$)			Weight loss %	
			Start	End	T_p	Partial	Total
S_1	1st	76.0	33	176	104	05.25	80.33
	2nd	85.50	176	381	269	75.08	
S_2	1st	76.15	37	156	94	06.75	69.39
	2nd	80.48	156	340	288	62.64	
S_3	1st	26.77	42	150	104	09.57	69.06
	2nd	68.96	150	338	299	59.49	
S_4	1st	11.73	43	200	48	07.32	52.21
	2nd	104.09	200	322	284	44.89	
S_5	1st	95.11	38	172	42	15.00	54.27
	2nd	49.96	172	327	289	39.24	

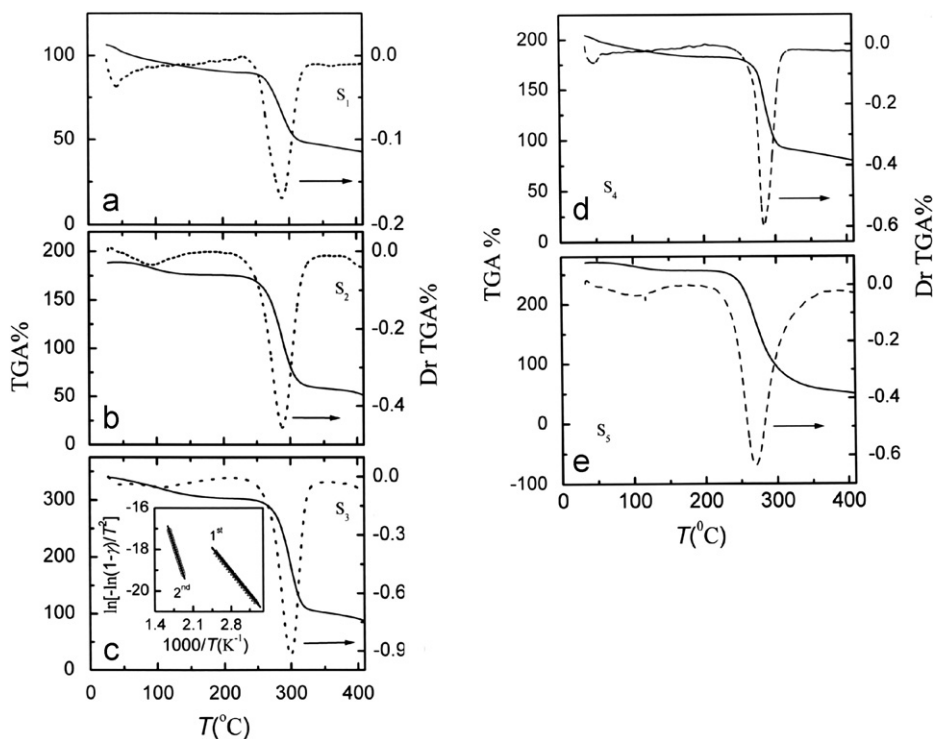


Fig. 3. (a–e): TGA% (left axis) and DrTGA% (right axis) for samples (a) S_1 , (b) S_2 and (c) S_3 , (d) S_4 and (e) S_5 . The inset in (c) shows the linear fit (solid lines) in the two decomposition steps of S_3 .

regions. It is to be noted that the peak temperature of the main degradation step is shifted to higher temperatures compared to pure PVA with increasing CMC content. This is an indication that CMC is more stable than PVA and the chemical structure plays an important role in the thermal decomposition process.

In order to obtain information about thermal stability of PVA/CMC blends, the activation energy (E) was calculated using Coats–Redfern's equation [30]:

$$\ln\left[\frac{-\ln(1-\gamma)}{T^2}\right] = -\frac{E}{RT} + \ln\left[\frac{AR}{\beta E}\left(1 - \frac{2RT}{E}\right)\right] \quad (4)$$

where A is a constant, β represents the heating rate, R is the universal gas constant and γ is the fraction of decomposition. Since the unit of E is in kJ/mol (see Table 3), $2RT/E \ll 1$, then Eq. (4) can be reduced to

$$\ln\left[\frac{-\ln(1-\gamma)}{T^2}\right] = -\frac{E}{RT} + \ln\left[\frac{AR}{\beta E}\right] \quad (5)$$

The plot of $\ln[-\ln(1-\gamma)/T^2]$ against $1/T$ should give a straight line whose slope is directly proportional to $-E/R$. For instance, the inset in Fig. 3(c) shows the linear fit in the two decomposition steps of S_3 according to Eq. (5). The values of E for all PVA/CMC blends in the first and second decomposition steps were calculated and listed in Table 3. It is clear from this table that E in the two decomposition steps changes irregularly in the individual polymers and their blend samples. Except for S_5 , the values of E of all the investigated samples in the first decomposition step are less than those in the second step. With increasing temperature, random scission of macromolecules predominates and then E exhibits pronounced changes. Based on Coats–Redfern's method, the values of E for some blends are comparable with those reported for cellulose acetate/niobium (CA/Nb) composites [31].

3.3. Dielectric properties

3.3.1. Dielectric permittivity

It is well known that the dielectric polarization in polymeric materials may be explained by rotation/motion of the dipole alignment, migration of ions within the matrix, or injection from electrodes. Fig. 4(a–d) shows the frequency dependence of the real part of the dielectric constant (ϵ') at some selected temperatures (below and above T_g) for all the blend samples. Within the studied range of frequency ($f=0.01$ –100 kHz), ϵ' decreases with increasing f . The decrease of ϵ' with frequency for all the samples at given temperature may be attributed to the decreasing number of dipoles, which contribute to polarization or the dipole structure is no longer able to respond to the applied electric field. It is worth noting that the magnitude of the frequency dispersion depends on the temperature, and the dielectric increment tends to become more pronounced as the temperature approaches T_g [32]. As seen from Fig. 4(a), S_1 exhibits a higher dielectric constant at $T \leq 323$ K but the effect of blending (PVA/CMC) appears on further increase in temperature. Moreover, ϵ' of S_1 is higher than that of S_5 while ϵ' of S_3 is near to that of S_5 . On the other hand, S_2 and S_4 exhibit higher dielectric constants at $T \geq 348$ K. Obviously, the behavior of $\epsilon'(f)$ depends on temperature and sample composition.

Fig. 5(a–c) depicts the temperature dependence of $\epsilon'(T)$ at some selected frequencies (1, 20, 100 kHz) for all the investigated samples. Focusing first on the homopolymers (S_1 and S_5), more than one peak was observed in $\epsilon'(T)$. The first peak for S_1 is located around 345 K and can be attributed either to the local main-chain dynamic or to different side group motions. The second peak is observed in the vicinity of T_g (360 K) [24,33,34] and can be associated to α -relaxation, which is of dipolar nature. Moreover, the height of the two peaks decreases with increasing frequency. With respect to CMC (S_5), $\epsilon'(T)$ also exhibits two peaks around temperatures 393, 407 K. While the first one corresponds to the crystalline state of this material, the second one is a non dipolar

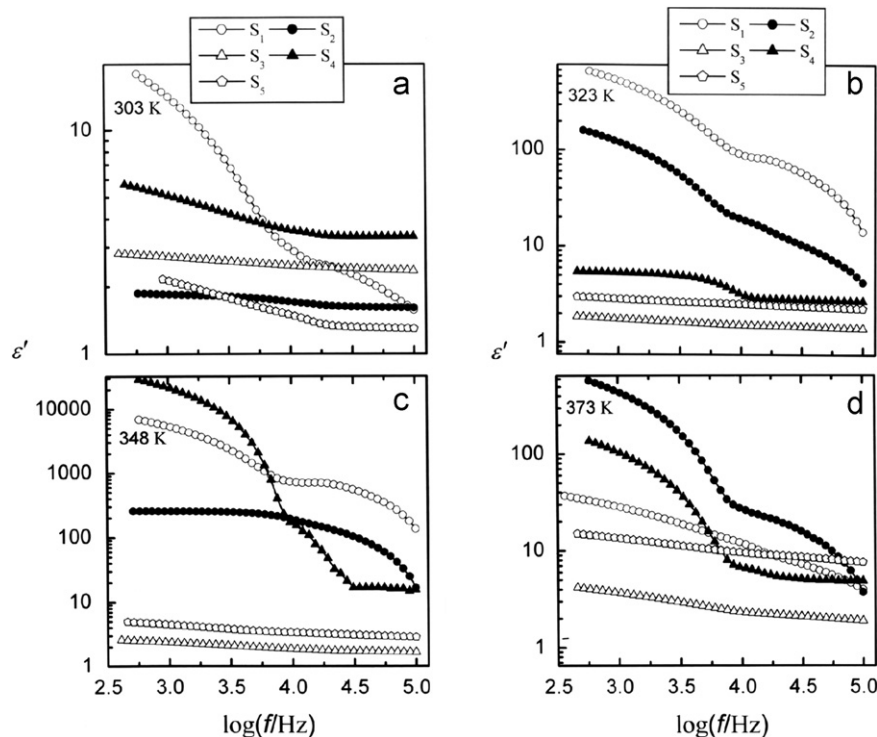


Fig. 4. Frequency dependence of ϵ' for all the samples at different temperatures; (a) $T=303$ K, (b) $T=323$ K, (c) $T=348$ K and (d) $T=373$ K.

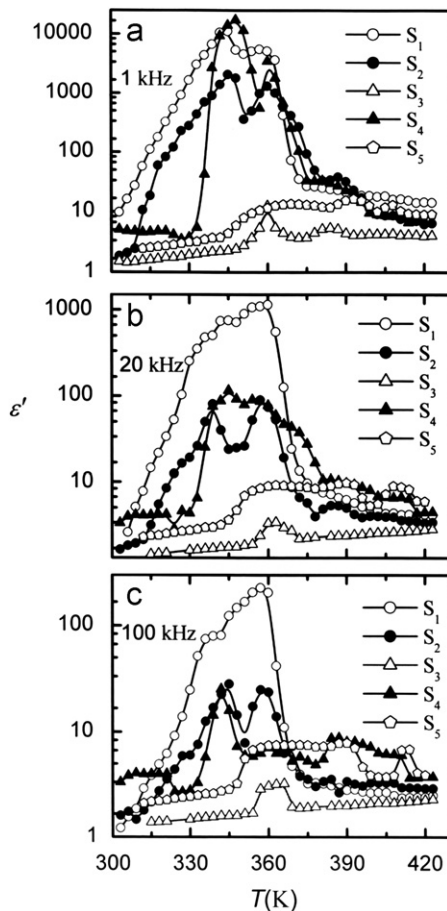


Fig. 5. Temperature dependence of ϵ' for all samples at different frequencies; (a) 0 kHz, (b) 20 kHz and (c) 100 kHz.

process and may be due to the interfacial polarization or space charge polarization effects [35]. Also, this peak is not always easily detected, but it is frequently associated with the onset of ionic conductivity processes, and therefore this process can be labeled as σ -relaxation. As in previous reports, one peak was observed in the $\epsilon'(T)$ curves of S_1 around 347 K [1]. This deviation may be related to adsorbed water molecules inside the polymer matrix, which reflects a higher dielectric constant. Also, the presence of water as solvent could modify self association of PVA and CMC. The behavior of $\epsilon'(T)$ depends on the PVA/CMC ratio. Similar to S_1 , two peaks can be distinguished for S_2 owing to the majority amount of PVA. In contrast, $\epsilon'(T)$ behavior of CMC is predominant for S_4 . When the ratio of PVA to CMC is equal (as in S_3), two indexed peaks at $f=1$ kHz are revealed while only one at higher frequencies ($f \geq 20$ kHz) is observed. This reveals that the compatibility of the prepared compositions depends on the homopolymers ratio. The samples S_1 , S_2 and S_4 show higher dielectric constant compared to those of other compositions. Moreover, the peak position and height of these three samples can be distinguished from that of S_3 and S_5 . The values of $\epsilon'(T)$ for S_3 are comparable with that of S_5 . This implies a similar behavior of $\epsilon'(f)$ and $\epsilon'(T)$ for these two samples. The temperature coefficient of permittivity (TCP) for all the samples at different frequencies is obtained using the relation

$$\text{TCP} = \frac{1}{\epsilon'} \frac{d\epsilon'}{dT} \quad (6)$$

where ϵ' is the value of the dielectric constant at the half maximum peak and $d\epsilon'/dT$ is the change of ϵ' with temperature. All values are

Table 4

The temperature coefficient of permittivity (TCP) for all samples.

Frequency	1 kHz	20 kHz	100 kHz
Sample	TCP (K^{-1})	TCP (K^{-1})	TCP (K^{-1})
S_1	0.051	0.056	0.067
S_2	0.047	0.056	0.048
S_3	0.035	0.042	0.042
S_4	0.044	0.048	0.051
S_5	0.035	0.039	0.041

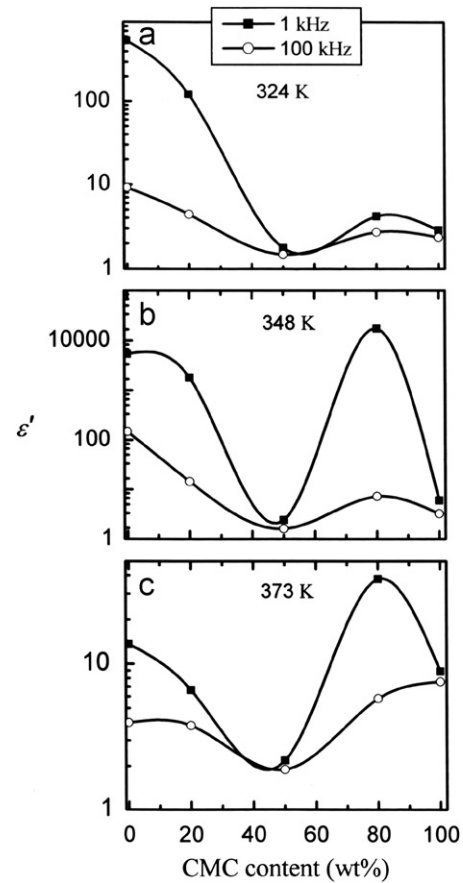


Fig. 6. Change of ϵ' with CMC content (wt%) at different temperatures; (a) 24 K, (b) 348 K and (c) 373 K.

listed in Table 4 and it may be noticed that TCP increases with increasing frequency and also depends slightly on the sample composition.

Fig. 6(a–c) represents the change of ϵ' with CMC content at different frequencies and at some selected temperatures. ϵ' decreases gradually with increasing CMC content at 324 K. A minimum at 50 wt% of CMC was observed in ϵ' with increasing temperature (373 K). Moreover, the concentrations 20 and 80 wt% of CMC show higher dielectric constants compared to the other blend samples. This behavior is consistent with $\epsilon'(T)$ of the investigated samples (see Fig. 5).

3.3.2. Dielectric loss tangent

The dielectric losses in most polymeric materials may be attributed to the perturbation of phonons by the application of the electric field and the energy is transferred to phonon dissipation in the form of heat. Blending of polymers modifies the perturbation of phonon during application of an electric field

[36,37]. Fig. 7(a–d) represents the frequency dependence of dielectric loss, $\tan \delta$, at some selected temperatures (303, 323, 348 and 373 K). The variation of $\tan \delta$ with frequency gives evidence for a very distinct dipolar peak whose position depends on the temperature and the PVA/CMC ratio. A distribution of molecular weights or a cooperative movement of adjacent chains could give rise to this spread in relaxation times. The existence of a peak at low frequency is an indication of the longer relaxation time pertinent to macromolecules. It may be seen that as the temperature increases, the maximum of $\tan \delta$ shifts toward higher frequencies and indicates dielectric relaxation of the dielectric losses [38,39]. These well-known features are characteristics of the freezing of dipolar motion with no long-range correlations (i.e. glass-like). The values of $\tan \delta$ as well as the position of relaxation peak depend on both temperature and sample composition. Also, the behavior of $\tan \delta$ for S_3 is similar to that of S_5 at $T > 303$ K. It is observed that the full width at half maximum changes appreciably in the frequency range investigated and yet it is different from the maximum breadth of the Debye peak (1.14 decades). Also, the full width at half maximum of the peak loss depends on the sample composition as well as the frequency range.

The relaxation process can be described by the Arrhenius relation

$$f = f_0 \exp(-E_r/kT) \quad (7)$$

where E_r is the activation energy for the relaxation process, f is the frequency of the loss peak maximum and f_0 is the characteristic constant parameter for a particular relaxation process. Plot of $\log(f_{max})$ versus $1000/T$ is shown in Fig. 8. The graph results in activation energies of $E_r \approx 0.04, 0.08, 0.33, 0.18$ and 0.07 eV for S_1, S_2, S_3, S_4 and S_5 , respectively. The relatively higher values of E for S_3 and S_4 blend samples signify an increase in binding forces, which oppose dipolar reorientation.

3.3.3. Ac conductivity (σ_{ac})

There are several models describing the origin and nature of charge carriers in polymeric chains, which take into account the

specific electronic structure of a given polymer. The lack of long-range order in most polymer systems does not allow for an extension of such treatments to completely describe their actual macroscopic electronic properties. Rather, the observed bulk conductivity of polymer system is a complex function of the number of charge carriers and their transport along polymer chains and morphological barriers. The ac conductivity measurements are important to characterize the nature of the conduction process.

For clarity, the double logarithmic plot of the frequency dependence of the real part of the ac conductivity at two selected temperatures is displayed in Fig. 9(a,b). As can be seen, each curve displays conductivity dispersion, which is strongly dependent on frequency and temperature. $\sigma'(f)$ increases monotonically with increasing frequency for the samples; S_2, S_3, S_4 and S_5 at $T=323$ K as seen in Fig. 9(a). On the other hand, $\sigma'(f)$ increases initially with frequency (up to 3 kHz) for all the samples at 373 K as shown in Fig. 9(b). While S_1 shows a higher conductivity at $T=323$ K, S_2 exhibits the highest values of $\sigma'(f)$ at $T=373$ K. Also the relaxation peak becomes broad with increasing CMC content and depends on temperature. This type of behavior reveals that the mechanisms responsible for ac conduction could be hopping. It is found to be consistent with that observed in many hopping systems

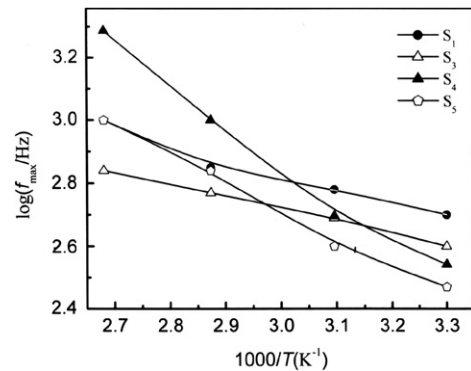


Fig. 8. Plot of $\log(f_{max})$ versus $1000/T$ for some selected samples.

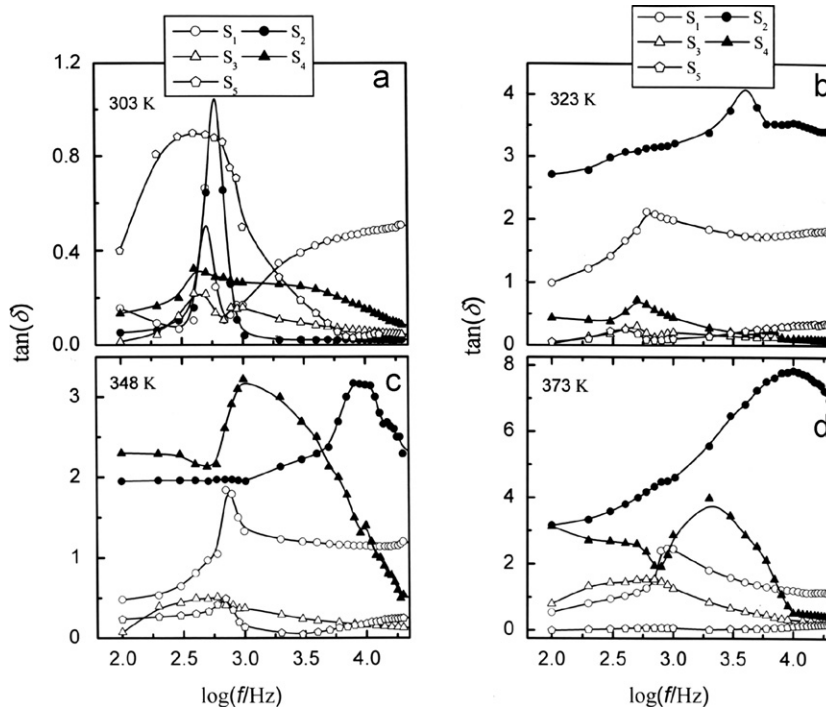


Fig. 7. Frequency dependence of $\tan \delta$ for all the samples at different temperatures; (a) $T=303$ K, (b) $T=323$ K, (c) $T=348$ K and (d) $T=373$ K.

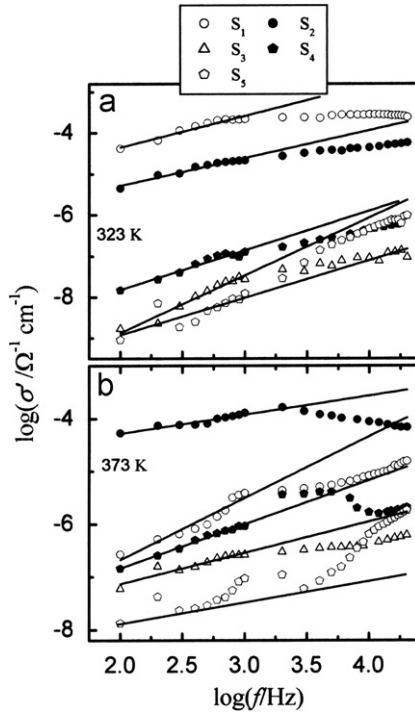


Fig. 9. Frequency dependence of the real part of the ac conductivity (σ') for all blends at different temperatures; (a) $T=323$ K and (b) $T=373$ K. The solid lines are the fitting according to Eq. 8.

Table 5

The values of the exponent s and the polaron binding energy (U_M) for PVA/CMC blends at different temperatures.

Sample	303 K		323 K		348 K		373 K	
	s	U_M (eV)						
S ₁	0.82	0.87	0.80	0.83	0.75	0.72	0.49	0.37
S ₂	0.88	1.3	0.31	0.24	0.26	0.24	0.19	0.23
S ₃	0.50	0.31	0.48	0.32	0.46	0.33	0.31	0.27
S ₄	0.50	0.31	0.49	0.32	0.45	0.32	0.41	0.32
S ₅	0.34	0.23	0.16	0.19	0.11	0.21	0.08	0.20

[39,40]. The real part of the ac conductivity, $\sigma'(f)$, can be described by the relation

$$\sigma'(f) = \sigma_{ac} - \sigma_{dc} = Df^s \quad (8)$$

where σ_{ac} is the dc (or low frequency) conductivity, σ_{dc} is the ac conductivity ($\sigma_{ac} = \omega \epsilon_0 \epsilon' \tan \delta$). The dc conductivity is subtracted by extrapolating σ_{ac} to the $f \rightarrow 0$ and then $\sigma'(f)$ is determined. D is constant and s is the exponent of the frequency. The above equation is valid for several low mobility polymers [41,42]. Based on Eq. 8, the plots of $\log(\sigma')$ versus $\log(f)$ yield straight lines of different slopes, i.e. of s . The values of s were derived within the range of frequency ($100 \text{ Hz} \leq f \leq 3 \text{ kHz}$), and tabulated in Table 5. The exponent s changes with increasing temperature and its value is less than unity i.e., $0 < s < 1$. This means that the values of s are in accordance with the theory of hopping conduction in amorphous materials at low frequencies [43,44]. Accordingly, these results lead to the prediction that the correlated barrier hopping (CBH) is the most suitable mechanism to explain the ac conduction behavior in the considered system [42]. In the CBH model [45,46], the exponent s was found to obey the form

$$s = 1 - \frac{6kT}{U_M - kT \ln(1/\omega\tau_0)} \quad (9)$$

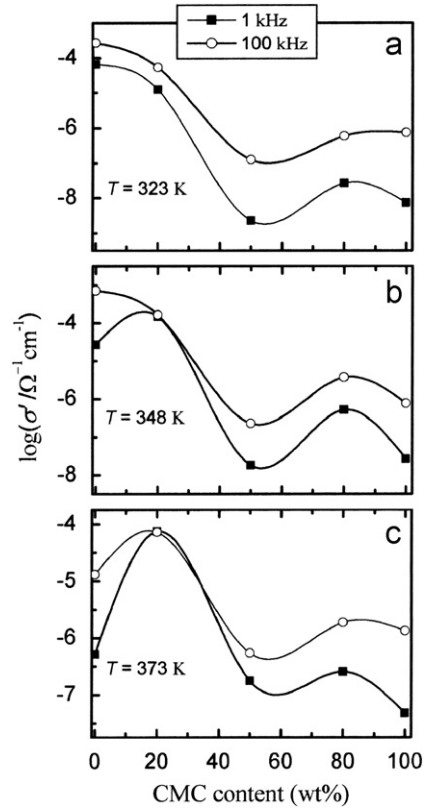


Fig. 10. Change of the real part of the ac conductivity (σ') against CMC content (wt%) at different temperatures; (a) 324 K, (b) 348 K and (c) 373 K.

where U_M is the maximum barrier height at infinite separation, which is called the “polaron binding energy”, i.e. the binding energy of the carrier in its localized sites and τ_0 is a characteristic relaxation time, which is in the order of an atom vibrational period ($\tau_0 \approx 10^{-13}$ s). The values of U_M at different temperatures are also given (Table 5). For large values of U_M/kT , the exponent s becomes [47]

$$s = 1 - \frac{6kT}{U_M} \quad (10)$$

To shed light on the change of the real part of the ac conductivity with composition, Fig. 10(a–c) shows $\log(\sigma')$ versus CMC content. As seen there is a change of ϵ' with CMC content, a similar trend is noticed for σ' . This means that σ' decreases with increasing CMC content up to 50% and exhibits a peak around 80 wt% of CMC. Again, the concentrations 20 and 80 wt% show higher ac conductivity as compared to other compositions. Also a minimum at 50 wt% composition is recognized in $\log(\sigma')$ at different temperatures similar to the behavior of ϵ' versus CMC content.

4. Conclusions

DSC shows that the blend system PVA/CMC is compatible within the studied range of compositions. TGA and DrTGA data show that there are two decomposition steps in the studied range of temperatures. The thermal stability of PVA/CMC blend samples is enhanced by increasing the CMC content. The composition 50/50 of PVA/CMC exhibits low absorption edge compared to other blend samples indicating that it has a higher carrier concentration in the localized levels. Dielectric dispersion of the investigated samples is found to occur in the audio frequency range. The dielectric constant

is frequency as well as temperature dependent. While $\varepsilon'(f)$ of all the samples decreases with increasing frequency due to the decrease of the number of dipoles, which contribute to polarization, the temperature dependence of dielectric permittivity, $\varepsilon'(T)$, exhibits more than one peak due to adsorbed water molecules inside the polymer matrix. Moreover, the calculated temperature coefficient of permittivity (TCP) for all the blends increases with increasing temperature and depends slightly on the content of CMC. Again, the composition 50/50 of PVA/CMC (wt/wt%) shows a minimum in ε' at different temperatures so it may be suitable for applications. Based on the frequency ac conductivity dependence at different temperatures, the correlated barrier hopping model (CBH) can be suggested for PVA, CMC and their studied blends.

Acknowledgment

The authors would like to acknowledge the financial support of Taif University, Kingdom of Saudi Arabia.

References

- [1] B.C. Shekar, V. Veeravazhuthi, S. Sakthivel, D. Mangalaraj, S.K. Narayandass, *Thin Solid Films* 348 (1999) 122.
- [2] E.H. Land, *J. Opt. Soc. Am.* 41 (1951) 957.
- [3] R. Bergman, L. Börjesson, L.M. Torell, A. Fontana, *Phys. Rev. B* 56 (1997) 11619.
- [4] D.Q.M. Craig, J.M. Newton, R.M. Hill, *J. Mater. Sci.* 28 (1993) 405.
- [5] E. Ikada, H. Fukushima, T. Watanabe, *J. Polym. Sci. Polym. Phys. Ed.* 17 (1978) 1789.
- [6] U. Kaatz, O. Gottmann, R. Podbielski, R. Pottel, U. Terveer, *J. Polym. Chem.* 82 (1987) 112.
- [7] V.R.K. Murthy, P.K. Kadaba, P.K. Bhagat, *J. Polym. Sci. Polym. Phys. Ed.* 17 (1979) 1485.
- [8] N.G. McCrum, B.E. Read, G. Williams, *Anelastic and Dielectric Effects in Polymeric Solids*, John Wiley & Sons, New York, 1967.
- [9] R.J. Sengwa, H.D. Purohit, *Polym. Int.* 29 (1992) 25.
- [10] A. Kyritsis, P. Pissis, J. Grammatikakis, *J. Polym. Sci. Polym. Phys.* 33 (1995) 1737.
- [11] J.-S. Park, J.-W. Park, E. Ruckenstein, *Polymer* 42 (2001) 4271.
- [12] B. Sarti, M. Scandola, *Biomaterials* 16 (1995) 785.
- [13] L.G. Allgen, S. Roswall, *J. Polym. Sci.* 12 (1954) 229.
- [14] R.J. Sengwa, K. Kaur, *Polym. Int.* 49 (2000) 1314.
- [15] B.C. Shekar, V. Veeravazhuthi, S. Sakthivel, D. Mangalaraj, S.K. Narayandass, *Thin Solid Films* 348 (1999) 122.
- [16] F.H. Abd El-Kader, A.M. Shehap, M.S. Abo-Elilil, K.H. Mahmoud, *J. Appl. Polym. Sci.* 95 (6) (2005) 1342.
- [17] P. Dutta, S. Biswas, M. Ghosh, S.K. De, S. Chatterjee, *Synth. Met.* 122 (2001) 455.
- [18] P. Banerjee, *Eur. Polym. J.* 34 (10) (1998) 1557.
- [19] A.S. Ibrahim, G. Attia, M.S. Abo-Elilil, F.H. Abd El-Kader, *J. Appl. Polym. Sci.* 63 (3) (1997) 343.
- [20] N.A. Peppas, E.W. Merrill, *J. Appl. Polym. Sci.* 20 (6) (1976) 1457.
- [21] F.H. Abd El-Kader, W.H. Osman, K.H. Mahmoud, M.A.F. Basha, *Physica B* 403 (2008) 3473.
- [22] F. Urbach, *Phys. Rev.* 92 (1952) 1324.
- [23] F.H. Abd El-Kader, S.A. Gaafar, K.H. Mahmoud, S.I. Bannan, M.F.H. Abd El-Kader, *J. Appl. Polym. Sci.* 110 (2008) 1281.
- [24] F.H. Abd El-Kader, A.M. Shehap, M.S. Abo-Elilil, K.H. Mahmoud, *J. Polym. Mater.* 22 (2005) 349.
- [25] Y. Nishio, R. John Manley St., *Macromolecules* 21 (1988) 1270.
- [26] H.E. Kissinger, *Anal. Chem.* 29 (1957) 1702.
- [27] N. Mehta, A. Kumar, *J. Optoelectron. Adv. Mater.* 7 (3) (2005) 1473.
- [28] Y.B. Saddeek, E.R. Shaaban, F.M. Abdel-Rahim, K.H. Mahmoud, *Philos. Mag.* 88 (25) (2008) 3059.
- [29] J. Tripathy, D.K. Mishra, K. Behari, *Carbohydr. Polym.* 75 (2009) 604.
- [30] A.W. Coats, J.P. Redfern, *Nature* 201 (1964) 68; A.W. Coats, J.P. Redfern, *J. Polym. Sci. B: Polym. Lett.* 3 (1965) 917.
- [31] E.A. Faria, A.G.S. Prado, *React. Funct. Polym.* 67 (2007) 655.
- [32] G.R. Saad, *Polym. Int.* 34 (4) (1994) 411.
- [33] P.D. Garrett, D.T. Grubb, *J. Polym. Sci. Part B: Polym. Phys.* 26 (12) (1988) 2509.
- [34] I. Scis, T.A. Ezquerra, F.T.B. Calleja, V. Tupererina, M. Kalnins, *J. Macromol. Sci. Phys.* 39 (2000) 761.
- [35] M.D. Migahed, N.A. Baker, M.I. Abdel-Hamid, D. El-Hanafy, M. El-Nimr, *J. Appl. Polym. Sci.* 59 (4) (1996) 655.
- [36] I.M. Talwar, H.C. Sinha, A.P. Shrivastava, *J. Mater. Sci. Lett.* 4 (1985) 448.
- [37] N. Chand, N. Khare, *Indian J. Pure Appl. Phys.* 38 (2000) 526.
- [38] L.O. Faria, R.L. Moreira, *J. Polym. Sci. Part B: Polym. Phys.* 37 (1999) 2996.
- [39] A.M. Saleh, R.D. Gould, A.K. Hassan, *Phys. Status Solidi (a)* 139 (21) (1993) 379.
- [40] R. Bahri, H.P. Singh, *Thin Solid Films* 62 (1979) 291; R. Bahri, H.P. Singh, *Thin Solid Films* 69 (1980) 281.
- [41] D. Nataraj, K. Senthil, S.K. Narayandass, D. Mangalaraj, *Cryst. Res. Technol.* 34 (1999) 867.
- [42] R.I. Mohamed, *J. Phys. Chem. Solids* 61 (8) (2000) 1357.
- [43] M. Pollak, T.H. Geballe, *Phys. Rev.* 122 (1961) 1742.
- [44] N. Balasundaram, D. Mangalaraj, S.K. Narayandass, C. Balasubramanian, *Phys. Status Solidi (a)* 130 (1992) 141.
- [45] I.G. Austin, N.F. Mott, *Adv. Phys.* 18 (1969) 657.
- [46] K.L. Nagai, *Comments Solid State Phys.* 9 (1979) 127.
- [47] G.E. Pike, *Phys. Rev. B* 6 (1972) 1572.